A COMPARISON OF THE BUGLE-80, SAILOR, AND ELXSIR NEUTRON CROSS-SECTION LIBRARIES FOR PWR PRESSURE VESSEL SURVEILLANCE DOSIMETRY AND SHIELDING APPLICATIONS

MATERIALS

KEYWORDS: *cross sections, pressure vessel dosimetry, light water reactors*

HASSAN S. BASHA *The Pennsylvania State University*
231 Sackett Building, University Park, Pennsylvania 16802

MICHAEL P. MANAHAN, Sr. *MPM Research & Consulting*
213 Teaberry Circle, State College, Pennsylvania 16803

Received November 4, 1991
Accepted for Publication April 21, 1992

Three multigroup neutron cross-section libraries are used in synthesized three-dimensional discrete ordinates transport analyses to investigate their similarities, differences, and results for pressurized water reactor (PWR) pressure vessel surveillance dosimetry and shielding applications. The accurate determination of the neutron energy spectra and key exposure parameters, such as the integrated fast flux and total displacement per atom (dpa) within the pressure vessel wall, is very important for surveillance capsule analysis, pressure vessel embrittlement calculations, pressure-temperature curve calculations, and plant life extension planning. The accuracy of any radiation transport analysis depends in part on the cross-section library used to model the various materials.

The calculated-to-experimental (C/E) ratios and the calculated reaction rates of several fast reactions are compared for the BUGLE-80, SAILOR, and ELXSIR cross-section libraries at the 97-deg surveillance capsule of the San Onofre Nuclear Generation Station Unit 2 (SONGS-2) and at the 90- and 97-deg (C/E ratios only) cavity dosimetry locations for another PWR (referred to as Reactor X). Additionally, the displacement per atom per second attenuation through the pressure vessel wall is compared with that of the integrated fast neutron flux ($E > 1.0$ MeV) and with the attenuation functions given in U.S. Nuclear Regulatory Commission Regulatory Guide 1.99, Revisions 1 and 2. Finally, the pressure vessel wall exposure sensitivity to fast neutrons due to vessel eccentricity and the buildup of ^{239}Pu in the core region are also reported.

The C/E ratios calculated using ELXSIR with the updated iron cross sections for SONGS-2 are fairly close to unity compared with those calculated using the other two cross-section libraries. The Reactor X C/E ratios are close to unity using the BUGLE-80 and SAILOR libraries and much higher than unity (~1.7) for ELXSIR with the updated iron cross sections at two cavity dosimetry locations (90 and 97 deg). The large C/E ratio is believed to be caused by vessel eccentricity. The ELXSIR cross-section library with the updated iron cross sections also produced much higher calculated reaction rates for both reactors.

The fast flux ($E > 1.0$ MeV) through the pressure vessel wall increases by 17% when the SONGS-2 core and core barrel are moved 1.27 cm closer to the pressure vessel wall to simulate vessel eccentricity. The fast flux also increases by as much as 10% for SONGS-2 and 15% for Reactor X when a mixed fission spectrum (plutonium and uranium) is used to model the neutron source in the core region. Finally, the two attenuation functions (fast flux and dpa) given in Regulatory Guide 1.99, Revisions 1 and 2, differed from the plant-specific calculation for both SONGS-2 and Reactor X.

Overall, ELXSIR is the best available cross-section library for broad multigroup light water reactor vessel calculations. This judgment is based primarily on the improved C/E ratios observed for both in-vessel and ex-vessel dosimetry experiments. However, the use of an improved cross-section library is not sufficient to ensure accurate flux and fluence data. Factors such as core, core barrel, and pressure vessel eccentricity can significantly affect the calculation of the magnitude of neutron damage parameters. Thus, reliable flux determination can only be ensured by continued use of dosimetry.

I. INTRODUCTION

Nuclear cross sections are an essential part of any reactor physics calculation. The ability to produce accurate results in these calculations depends in part on the cross-section library used to represent the various materials within the reactor. Other factors that contribute to the accuracy of the results include vessel, core, and thermal shield eccentricity; the ability to model various components in the as-built configuration; precise capsule location; accurate description of the source distribution and power history; and the variation of the pressure vessel cladding thickness.

Since nuclear cross sections usually have complicated dependence on neutron energy and scattering angle, factors such as the energy group structure, the order of the angular scattering expansion, and verification against experimental data are very important in determining whether a particular cross-section library is suitable for the calculations of interest. This is of particular importance in light water reactor (LWR) pressure vessel shielding problems. Since the pressure vessel wall, core internals, and support structures are subject to mechanical property degradation induced by neutron leakage from the core,[1,2] the integrity of these components must be evaluated by developing damage models that are a function of critical exposure parameters.

One reliable and cost-effective approach is to perform discrete ordinates neutron transport analyses to determine the neutron spectra and flux at critical locations. Then, the analytically determined neutron spectra are combined with dosimetry measurements using the foil activation technique[3,4] or a recently developed material scrapings technology[5] to determine the pseudo fluxes. The material scrapings approach can be very valuable to nuclear utilities through end of license and, more importantly, during the plant life extension period because it can generate fluence and mechanical property data for various in-service components without removing them from service.

Since the objective of any reactor physics analysis is to produce the most accurate results to the extent practical, it is essential that the best available and most suitable cross-section library be used. The BUGLE-80 (47 neutron, 20 gamma, P_3) (Ref. 6), SAILOR (47 neutron, 20 gamma, P_3) (Ref. 7) (Shielded and Application Independent Libraries for Operating Reactors) and ELXSIR (56 neutron, P_3) (Ref. 8) (EPRI LWR X-Sections for IRradiation Studies) are multigroup cross-section libraries that were developed specifically for LWR dosimetry and shielding applications. In this study, two dimensional *S-N* neutron transport calculations (r-θ, r-z) were performed for the San Onofre Nuclear Generation Station Unit 2 (SONGS-2) and Reactor X plants using the three cross-section libraries. The SONGS-2 plant was chosen because it is a recently built pressurized water reactor (PWR) with adequate in-vessel spectral dosimetry data. Reactor X was chosen because it has extensive ex-vessel dosimetry data. Reactor X is a PWR power plant currently operating in the United States. Since the flux and dosimetry data are proprietary, we present only normalized data for this plant. Then the synthesized three-dimensional neutron fluxes and energy spectra were calculated by combining the results of the r-θ and r-z transport analyses. The results were then compared against measured data, and conclusions are drawn concerning the "goodness" of each cross-section library for pressure vessel wall surveillance dosimetry and shielding problems.

II. BACKGROUND

Over the past two decades, several multigroup cross-section libraries have been used in LWR shielding problems. However, most of these libraries were either not designed for LWR shielding problems and pressure vessel dosimetry analysis or were inappropriate for such calculations. For example, the DLC-23/CASK (22 neutron, 18 gamma) library,[9] which was designed for shipping casks, was extensively used throughout the nuclear industry in the past for LWR shielding calculations. This library was produced from ENDF/B-II neutron cross-section data and DLC-12/POPLIB (Ref. 10) gamma-ray production data and produced higher flux data than expected. Several multigroup libraries were created such as DLC-31/FEWG1 (37 neutron, 21 gamma) (Ref. 11), which was sponsored by the U.S. Defense Nuclear Agency, and a (27 neutron, 18 gamma) library based on DLC-43/CSRL (Ref. 12) developed for the U.S. Nuclear Regulatory Commission[13] (NRC). However, none of these newer libraries were specifically designed for LWR shielding applications and, thus, were considered inappropriate for such calculations. The suitability of a cross-section library

for a particular analysis can be determined when its results are benchmarked against experimental data.

The limited supply of coupled, multigroup cross-section libraries designed for LWR pressure vessel surveillance dosimetry and shielding analysis led the American Nuclear Society 6.1.2 working group to establish a set of standards for developing such libraries.[14] The DLC-47/BUGLE (45 neutron, 16 gamma) library[15] was the first attempt at developing such a library. This library was produced from the DLC-41/VITAMIN-C (171 neutron, 36 gamma) fine-group library.[16] Comparisons of BUGLE results with other multigroup libraries revealed deficiencies that limited its usefulness.[7] The spectrum used in generating BUGLE from the fine-group library contained features of both fission and fusion spectra that resulted in larger within-group scattering cross sections at higher energies than would be expected in LWRs. This resulted in overprediction of the fast neutron fluxes at the surface of the pressure vessel wall.

As a result of the experience gained using BUGLE, the DLC-75/BUGLE-80 (47 neutron, 20 gamma), DLC-76/SAILOR (47 neutron, 20 gamma), and ELXSIR (56 neutron) libraries were developed. The BUGLE-80 library was prepared using a PWR concrete-weighted spectrum for collapsing from the VITAMIN-C fine-group structure (171 neutron, 36 gamma) to a coarse-group structure (47 neutron, 20 gamma). SAILOR was prepared using more appropriate and spatially dependent spectra for collapsing from VITAMIN-C. On the other hand, ELXSIR was generated primarily to serve as the DOT-IV standard library in the LEPRICON system. This library was designed specifically for LWR fast neutron deep-penetration problems and was prepared from the 171-group VITAMIN-C library using regionwise weighting spectra typical of LWR plants.

III. SYNTHESIZED THREE-DIMENSIONAL NEUTRON SPECTRA AND FLUX CALCULATIONS

The synthesized three-dimensional neutron flux and spectra were calculated for SONGS-2 and Reactor X at the pressure vessel peak position (axial and azimuthal) for the pressure vessel inner wall surface, $\frac{1}{4}$ thickness T, $\frac{3}{4}T$, outer wall surface, and the cavity region. The integrated synthesized three-dimensional neutron fluxes were calculated for energies >0.1 and 1.0 MeV at these locations. American Society for Testing and Materials (ASTM) standards[17] were followed to the extent possible for the calculations of the neutron flux and spectrum. The cross-section preparation and the synthesized three-dimensional neutron transport calculative details are discussed below.

III.A. Cross-Section Preparation

The GIP (Group Organized Cross Section Input Program) computer code[18] was used for neutron cross-section preparation. The GIP code prepares a group-organized file of microscopic and/or macroscopic cross sections for multidimensional discrete ordinates codes. GIP treats each component of the Legendre expansion as a separate nuclide. The code input consists mainly of the material number densities for each mixture.

III.A.1. Bugle-80 Library

The BUGLE-80 cross-section library consists of 47 neutron and 20 gamma-ray energy groups and utilizes the P_3 Legendre expansion for calculating the particle angular scattering distribution. This library was produced using a PWR concrete spectrum to collapse from the fine-group library VITAMIN-C (171 neutron, 36 gamma) to (47 neutron, 20 gamma). Figure 1 shows the 171-energy-group neutron spectra that were used to prepare the BUGLE-80 and SAILOR cross-section libraries. It is important to note that BUGLE-80 is actually a subset of SAILOR. BUGLE-80 was published by Oak Ridge National Laboratory (ORNL) as a result of the standards established by the ANS 6.1.2 working group. Table I shows the neutron energy structures of the BUGLE-80, SAILOR, and ELXSIR libraries. BUGLE-80 contains a total of 72 materials (67 nuclei, 5 materials).

The SONGS-2 reactor was divided into nine regions including fuel, shroud, water inside the core barrel, core barrel, water in downcomer, surveillance capsule, low-carbon steel pressure vessel wall, air cavity, and concrete shield. The reactor core was modeled as ten homogenized fuel mixtures with different ^{235}U enrichments representing the different fuel assemblies. Each fuel assembly was homogenized by volume fraction

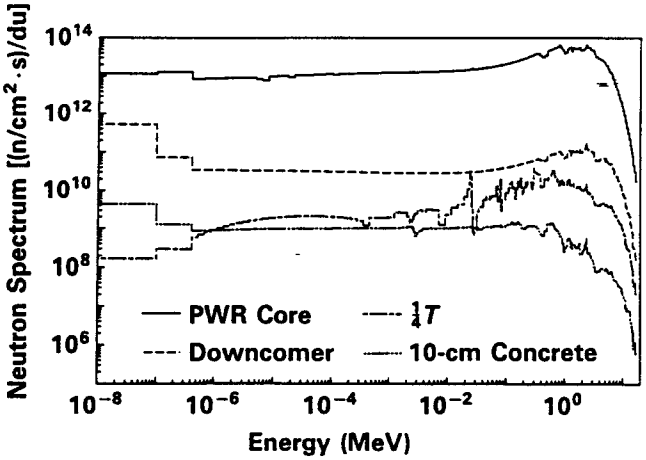

Fig. 1. ORNL 171-energy-group neutron spectra used in preparing BUGLE-80 and SAILOR cross-section libraries.

TABLE I

BUGLE-80, SAILOR, and ELXSIR Energy Group Structure

Neutron Energy Group Number	47-Group Structure		56-Group Structure	
	Upper Limit (MeV)	Lower Limit (MeV)	Upper Limit (MeV)	Lower Limit (MeV)
1	17.3300	14.1910	17.3300	14.1910
2	14.1910	12.2140	14.1910	12.2140
3	12.2140	10.0000	12.2140	11.0520
4	10.0000	8.60710	11.0520	10.0000
5	8.60710	7.40820	10.0000	8.60710
6	7.40820	6.06530	8.60710	8.18730
7	6.06530	4.96590	8.18730	7.40820
8	4.96590	3.67880	7.40820	7.04690
9	3.67880	3.01190	7.04690	6.06530
10	3.01190	2.72530	6.06530	4.96590
11	2.72530	2.46600	4.96590	4.06570
12	2.46600	2.36530	4.06570	3.67880
13	2.36530	2.34570	3.67880	3.01190
14	2.34570	2.23430	3.01190	2.72530
15	2.23430	1.92050	2.72530	2.59240
16	1.92050	1.65300	2.59240	2.46600
17	1.65300	1.35340	2.46600	2.36530
18	1.35340	1.00260	2.36530	2.34570
19	1.00260	0.82085	2.34570	2.23130
20	0.82085	0.74274	2.23130	2.12240
21	0.74274	0.60810	2.12240	1.92050
22	0.60810	0.49787	1.92050	1.82680
23	0.49787	0.36883	1.82680	1.65300
24	0.36883	0.29720	1.65300	1.49570
25	0.29720	0.18316	1.49570	1.35340
26	0.18316	0.11109	1.35340	1.22460
27	0.11109	0.06738	1.22460	1.00260
28	0.06738	0.04087	1.00260	0.90718
29	0.04087	0.03183	0.90718	0.82085
30	0.03183	0.02606	0.82085	0.74274
31	0.02606	0.02418	0.74274	0.60810
32	0.02418	0.02187	0.60810	0.49787
33	0.02187	0.01503	0.49787	0.36883
34	0.01503	0.00710	0.36883	0.30197
35	0.00710	0.00335	0.30197	0.21280
36	0.00335	0.00158	0.21280	0.18316
37	1.585E−03[a]	4.540E−04	0.18316	0.11109
38	4.540E−04	2.144E−04	0.11109	0.09804
39	2.144E−04	1.013E−04	0.09804	0.08652
40	1.013E−04	3.727E−05	0.08652	0.06738
41	3.727E−05	1.068E−05	0.06738	0.04007
42	1.068E−05	5.043E−06	0.04007	0.03437
43	5.043E−06	1.855E−06	0.03437	0.02606
44	1.855E−06	8.764E−07	0.02606	0.02418
45	8.764E−07	4.140E−07	0.02418	0.02187
46	4.140E−07	1.000E−07	0.02187	0.01503
47	1.000E−07	1.000E−11	0.01503	0.01171
48			0.01171	0.00071
49			7.101E−03	5.531E−03
50			5.531E−03	3.355E−03
51			3.355E−03	2.612E−03
52			2.612E−03	1.585E−03
53			1.585E−03	1.101E−04
54			1.101E−04	1.068E−04
55			1.068E−04	4.140E−07
56			4.140E−07	1.000E−11

[a]Read as 1.585×10^{-3}.

of the fuel pellet (^{238}U, ^{235}U, and ^{16}O), cladding material, B_4C-Al_2O_3 absorber rods, and core coolant at an average core temperature of 583°F at an operating pressure of 2250 psia (hydrogen and ^{16}O). The water in the downcomer region outside the core barrel had a density consistent with the inlet coolant temperature (553°F) and an operating pressure of 2250 psia. The coolant carried boron in solution at an average concentration of 462 g B/10^6 g of water for cycles 1, 2, and 3 (^{10}B and ^{11}B). The boron concentration was averaged over the three cycles by burnup weighting the average boron concentration of each cycle. The core shroud and core support barrel and vessel liner are Type 304 stainless steel. The reactor pressure vessel wall is an ASTM A533B steel. The air cavity between the pressure vessel wall and the concrete shield was modeled as ^{16}O and ^{14}N. The concrete shield is composed of hydrogen, carbon, oxygen, sodium, magnesium, aluminum, silicon, potassium, calcium, and iron. The 97-deg surveillance capsule (7-deg octal equivalent) was modeled as seven mixtures: Fe/Al, Cu/Al, Ni/Al, Ti/Al, and Co/Al for the dosimetry; ASTM A533B steel for the test specimens; and aluminum for the dosimetry spacers.

Similarly, Reactor X was divided into nine regions including fuel, shroud, water inside the core barrel, core barrel, water in downcomer, low-carbon steel pressure vessel wall, air cavity and ex-vessel dosimetry, and concrete shield. The ex-vessel dosimetry was located in the reactor cavity at octal equivalent locations of 0, 7, 13, 16, 40, and 45 deg. The reactor core was modeled as homogenized fuel rods, $UO_2Gd_2O_3$ shim rods, B_4C-Al_2O_3 absorber rods, and water. The core shroud, core support barrel, and vessel liner are Type 304 stainless steel. The reactor pressure vessel wall is ASTM A533B steel. The water in the core region has a density consistent with the average coolant temperature in the core (574°F) at an operating pressure of 2250 psia. The water in the downcomer region outside the core barrel has a density consistent with the inlet coolant temperature (550°F) and an operating pressure of 2250 psia. The water carried boron at an average concentration of 506 g B/10^6 g of water.

III.A.2. SAILOR Library

The SAILOR library contains 47 neutron energy groups and 20 gamma-ray energy groups with energy structure identical to that of BUGLE-80 (see Table I). SAILOR was developed specifically for LWR shielding and pressure vessel dosimetry applications. While BUGLE-80 was prepared using a PWR concrete spectrum, SAILOR was created using more appropriate spectra that represent the spatial location of materials present within the plant. These spectra include PWR core spectra, PWR downcomer spectra, PWR $\frac{1}{4}T$ spectra, and PWR concrete spectra (see Fig. 1).

SAILOR contains 58 materials (44 nuclei, 14 materials) that are most likely present in LWRs. The premixed materials include Type 304 stainless steel, ASTM A533B low-carbon steel, A508 CL2 steel, and ANSI standard concrete type 4. SAILOR also includes eight premixed fuel mixtures with varying ^{235}U enrichments.

The cross-section preparation procedures with SAILOR were similar to those of BUGLE-80 for both reactors. For example, the SONGS-2 reactor model contained ten fuel mixtures, water in core region, water in the downcomer, Type 304 stainless steel, pressure vessel A533B steel, air cavity, concrete shield, core shrould and core support barrel, and seven capsule mixtures. The same elements and number densities were used in preparing the cross sections for the fuel, water, air cavity, concrete shield, and the surveillance capsule mixtures. The elemental cross sections were chosen according to the location of the material. For instance, in modeling the core region, we used the microscopic cross sections for the fuel and water that were generated using the core spectrum. However, with regard to the pressure vessel A533B steel and Type 304 stainless steel liner, we used the premixed macroscopic cross sections for these materials. These mixtures were prepared using appropriate microscopic cross sections and number densities. While SAILOR contains most of the important nuclei needed to model these materials, it does not include several minor elements, such as copper, titanium, calcium, ^{11}B, ^{59}Co, and ^{14}N, that were used in our SONGS-2 BUGLE-80 model. Thus, for the completeness of our study, these elements were extracted from BUGLE-80 and added to SAILOR, even though they were found at very low concentrations ($\sim 10^{-6}$ atom/b·cm). This was done to ensure proper comparison between the two libraries.

III.A.3. ELXSIR Library

The ELXSIR library contains 56 neutron energy groups. It contains more energy groups than BUGLE-80 or SAILOR in the energy region between 0.1 and 10 MeV (see Table I). Similar to BUGLE-80 and SAILOR, this library uses the P_3 Legendre approximation for the angular scattering kernel. ELXSIR was developed specifically for LWR shielding and pressure vessel dosimetry applications. This library was produced from the VITAMIN-C fine-group library. Several nuclides in ELXSIR were prepared using VITAMIN-E (174 neutron, 38 gamma) (Ref. 19), which is derived from ENDF/B-V. The regionwise weighting spectra used in the collapsing process were generated from a one-dimensional transport analysis of a typical LWR (Arkansas Nuclear One Unit 1). Table II compares the radial dimensions of the SONGS-2 and Reactor X models with SAILOR and ELXSIR PWR reference models.

The ELXSIR cross-section library contains an additional set of updated iron cross sections for stainless steel and low-carbon steel. These updated iron cross

TABLE II

Radial Dimensions for SONGS-2 and Reactor X and SAILOR and ELXSIR Reference PWR Models

Reactor Region	SONGS-2	Reactor X	SAILOR Reference	ELXSIR Reference
Core outer radius	181.76	181.73	168.51	163.76
Flow baffle outer radius	185.75	184.88	171.40	166.46
Core barrel inner radius	187.96	188.60	187.96	179.07
Core barrel outer radius	195.58	193.04	193.68	184.15
Pressure vessel inner radius	220.98	218.34	219.71	217.17
Pressure vessel outer radius	242.89	241.09	241.62	239.08
Primary shield	358.15	335.28	360.00	345.44

sections were generated by Fu and Hetrick from ENDF/B-V Mod-3 (Ref. 20) and are considered to be the best broad multigroup iron cross sections available in a working format suitable for the ANISN or DOT transport codes. Both the original and updated sets of iron cross sections were used in our analyses. In this paper, we use the term ELXSIR-OLD when referring to the ELXSIR library with the original iron cross sections and the term ELXSIR-NEW to refer to the ELXSIR library with the updated iron cross sections.

The ELXSIR library contains 47 different materials (36 nuclei and 11 compositions). The cross-section preparation procedures with ELXSIR were similar to those of BUGLE-80 and SAILOR for each reactor. The same elements and number densities were used in preparing the cross sections for the fuel, water, air cavity, concrete shield, and surveillance capsule mixtures.

III.B. Synthesized Three-Dimensional Neutron Transport Analysis

The energy and spatial distribution of the neutron flux were calculated using the DOT 4.3 computer program.[18] DOT solves the Boltzmann transport equation in two-dimensional geometry using the method of discrete ordinates. Balance equations are solved for the density of particles moving along discrete directions in each cell of a two-dimensional mesh. An S_8 angular quadrature was used, i.e., neutrons travel in 48 directions (24 positive and 24 negative). Both r-θ and r-z calculations were performed for each reactor. Since >2000 meshes were modeled in the core region alone for each reactor, the FMAT computer code[21] was used to determine what material lies in each core mesh. Figures 2 and 3 show the r-θ models used in the analyses for SONGS-2 and Reactor X, respectively.

The number of neutrons per cubic centimetre per second originating in each mesh is proportional to the power generated in that mesh. Power generation in the meshes was calculated for both the r-θ and r-z DOT runs based on the number of pins whose centers lay in each mesh and on the power in these pins. The PINPOW computer code[21] was used to perform these calculations. The relative pin powers were that of the PDQ depletion analysis supplied by each utility. The pin and axial powers of each assembly were first averaged over each depletion step for all cycles of interest using burnup weighting. Then, each cycle-averaged pin power was averaged over all cycles by burnup weighting each cycle.

Since the pin power model locates pin power centers and assigns pins to the appropriate meshes, an analysis was performed to estimate the maximum uncertainty introduced in this approach. For the meshing used in our analyses, at most 48% of the pins could potentially be affected by the PINPOW approximation. If the pin centers were located at the mesh corners, then the maximum effect on the fast flux due to source redistribution would be 1.8%. Therefore, this approximation is judged to have negligible effects on the flux prediction accuracy.

The PDQ data were also used to obtain burnup weighting factors for the determination of nu_{eff} and to calculate the effective fission spectrum. Two effective fission spectra are used in our analyses to model the neutron source in the core region. One was a pure ^{235}U fission spectrum while the second one was a mixed fission spectrum that accounted for the buildup of ^{239}Pu in the core region. These analyses were performed to determine the impact of the buildup of ^{239}Pu in the core region on the calculated fast flux through the pressure vessel wall.

To determine a three-dimensional flux, separability was assumed and the results of the DOT r-θ and r-z runs were synthesized. If we let

$$\phi(r,z,\theta) = C(r)\phi(r,\theta)\psi(r,z) \quad (1)$$

and require for θ normalization that

$$\frac{\int_0^{2\pi} \phi(r,z,\theta)\, d\theta}{\int_0^{2\pi} d\theta} = \psi(r,z) , \quad (2)$$

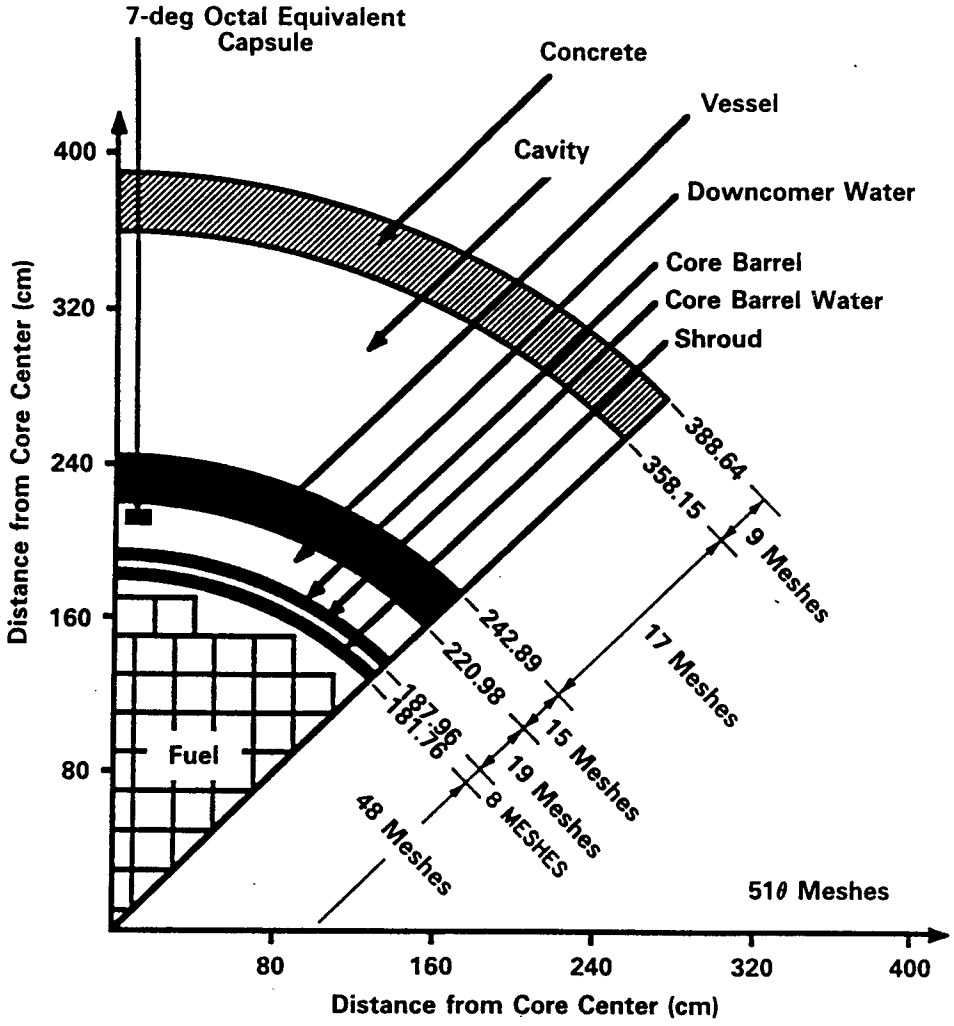

Fig. 2. SONGS-2 r-θ neutron transport model.

then

$$\frac{\int_0^{2\pi} C(r)\phi(r,\theta)\psi(r,z)\,d\theta}{2\pi} = \psi(r,z) \qquad (3)$$

and

$$C(r) = \frac{2\pi}{\int_0^{2\pi} \phi(r,\theta)d\theta} \,. \qquad (4)$$

In the case of z normalization, it was required that

$$\frac{\int_0^{z} \phi(r,z,\theta)\,dz}{\int_0^{z} dz} = \phi(r,\theta) \,, \qquad (5)$$

then

$$\frac{\int_0^{z} C(r)\phi(r,\theta)\psi(r,z)\,dz}{Z} = \phi(r,\theta) \qquad (6)$$

and

$$C(r) = \frac{Z}{\int_0^{z} \psi(r,z)dz} \,. \qquad (7)$$

The FLUX3DSYN computer code,[21] which reads the DOT output files, was used to perform the numerical integration of Eq. (7). This code also synthesized the fluxes at specific positions. As described in Ref. 5, the best geometric representation can be obtained using the z normalization model. The models described in this

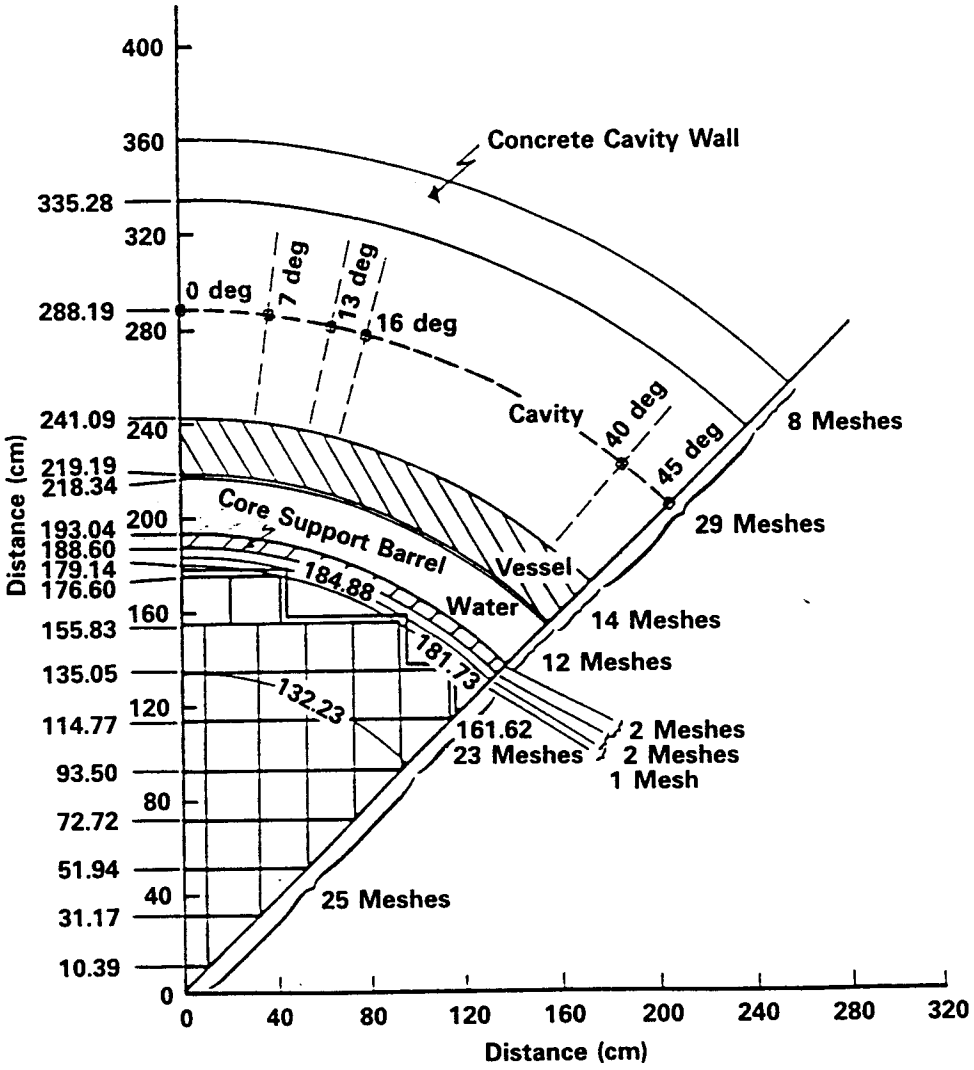

Fig. 3. Reactor X r-θ neutron transport model.

paper for synthesizing the three-dimensional flux distribution are similar to those given in Refs. 22 and 23.

The newly generated iron displacements per atom (dpa) cross sections in SAND-II (620-energy-group structure[24]), based on ENDF/B-VI iron cross sections, were compared against those given in ASTM STP-E693 (Ref. 25). Additionally, the new iron dpa cross sections were collapsed to the ELXSIR 56-energy-group structure using the Watt spectrum and were compared with those given in the ELXSIR library. Moreover, the pressure vessel wall attenuation of several key exposure parameters, such as total dpa per second, fast flux ($E > 1.0$ MeV), and the two attenuation functions proposed in Regulatory Guide 1.99, Revisions 1 and 2 (Ref. 26), are compared for each reactor. The "fast flux equivalent" attenuation function in Revision 1 is

$$f = f_{surface} * \exp(-0.33 * t) \ , \qquad (8)$$

where t is the wall depth in inches. The "dpa equivalent" attenuation function in Revision 2 has an exponent factor of 0.24.

III.C. Empirical Determination of Flux

In a dosimeter irradiation experiment, the parameter that is actually measured is the activity of the dosimeter rather than the flux. To infer the flux from the activity, it is necessary to know the energy dependence of the dosimeter cross section, the energy dependence of the flux at the dosimeter location, and the reactor operating history. In this study, neutron transport analyses were performed that could be used to estimate the neutron energy spectra at the dosimeter locations. Thus, the "measured" or "pseudo fluxes" described in this paper are actually a combination of a measured

activity and an analytically determined effective cross section from which the flux is determined. The pseudo flux, accounting for decay between exposure and counting as well as power level fluctuation, is given by

$$\phi(E > E_c) = \frac{A}{N\sigma(E > E_c)C} , \quad (9)$$

where

$$C = \sum_{n=1}^{K} f_n [1 - \exp(-\lambda t_i^n)] \exp(-\lambda t_w^n)$$

K = number of time intervals of constant flux

f_n = fractional power level during interval n

t_i^n = time length of the interval n irradiation

t_w^n = time between the end of interval n and counting

A = measured specific activity

E_c = cutoff energy

N = atom density of target nuclei

$\sigma(E > E_c)$ = effective cross section:

$$\sigma(E > E_c) = \frac{\int_0^\infty \sigma(E)\phi(E)\,dE}{\int_{E_c}^\infty \phi(E)\,dE} .$$

To determine the effective cross section $\sigma(E > E_c)$ to be used in these calculations, the cross section as a function of energy must be known. The DOSDAM84 640-group dosimetry cross-section library[27] based on ENDF/B-V data was used for this purpose. A modified version of the DETAN code was used in the analysis to collapse the 640-group cross sections to BUGLE-80 47-group structure to be used in the BUGLE-80 analysis. In the case of SAILOR and ELXSIR, dosimetry cross-section files were provided in each library and, thus, were used in our analysis. The daily reactor operating history data supplied by each utility were used to compute the saturated activities of each dosimeter.

IV. RESULTS

The radial distributions of the synthesized three-dimensional fast neutron fluxes ($E > 0.1$ and 1.0 MeV) were calculated at the pressure vessel peak position (axial and azimuthal) using the BUGLE-80, SAILOR, and ELXSIR libraries, respectively, for SONGS-2 and Reactor X. The synthesized three-dimensional neutron spectra were also calculated at several radial positions including the pressure vessel inner wall surface, $\frac{1}{4}T$, and outer wall surface. These positions were chosen because of their significance for reactor pressure vessel embrittlement calculations and because they also represent a wide range of spectral changes. The calculated-to-experimental (C/E) ratios for several threshold reactions were calculated using the three cross-section libraries for the 97-deg (near core midplane) in-vessel surveillance capsule of SONGS-2 and for the 90-deg (near core midplane) and 97-deg (~81 cm above core midplane) ex-vessel dosimetry locations of Reactor X. Additionally, the reaction rates for six fast threshold reactions were calculated using the three cross-section libraries for the 97-deg capsule of SONGS-2 and the 90-deg cavity dosimetry of Reactor X.

IV.A. SONGS-2 Transport Results

The synthesized three-dimensional fast fluxes with energies >1.0 and 0.1 MeV obtained using SAILOR were nearly identical (about <0.5%) to those obtained using BUGLE-80 out to the pressure vessel inner wall surface (220.98 cm), while the SAILOR-calculated fast fluxes were 1.0 and 5.5% higher at the pressure vessel outer wall surface, respectively. The SAILOR and BUGLE-80 results were in good agreement out to the pressure vessel inner wall surface primarily because the core and downcomer spectra that were used to generate the SAILOR library have a shape similar to the concrete spectrum that was used to develop the BUGLE-80 library in the fast energy range (i.e., 0.1 MeV < E < 17.33 MeV). The ORNL PWR core, downcomer, and concrete spectra are compared in Fig. 1. The radial distributions of the fast fluxes for energies >1.0 and 0.1 MeV at the pressure vessel peak position (axial and azimuthal) for the three cross-section libraries are shown in Fig. 4.

The difference in the fast flux through the pressure vessel wall is due to the fact that the pressure vessel cross sections in SAILOR were generated using a PWR $\frac{1}{4}T$ weighting spectrum compared to the PWR concrete spectrum that was used to generate BUGLE-80. This spectral effect was also evident when the concrete spectrum was used to collapse iron, carbon, and manganese cross sections for the SAILOR library. It is important to note that the resonance self-shielding that was used in the SAILOR library generating process had a negligible effect on the fast flux calculations.

In the case of the ELXSIR cross-section library, the calculated fast fluxes ($E > 1.0$ and 0.1 MeV) were considerably higher than those calculated using the BUGLE-80 library for both the original and updated iron cross sections. In the case using the original iron cross sections, the calculated fast fluxes for both energy cutoffs were ~8 and 9% higher in the core region,

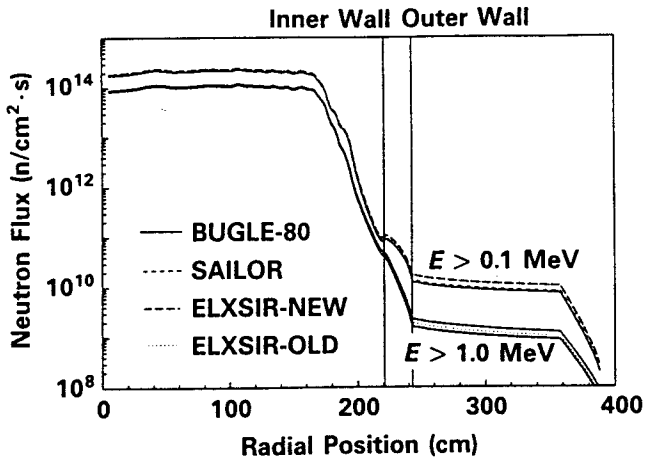

Fig. 4. Radial profile of the SONGS-2 synthesized three-dimensional neutron flux ($E > 1.0$ and 0.1 MeV) at pressure vessel peak position.

and in the core barrel and downcomer regions, respectively. The fast flux was considerably higher in the core region partly because of a small increase in the capture cross sections at high energy. This is most likely caused by the weighting spectrum that was used to generate ELXSIR and the fact that more energy groups were added in the energy range between 0.1 and 10 MeV. More importantly, the 56-energy-group fission spectrum that was used to model the neutron source in the core region was slightly harder than the corresponding 47-energy-group fission spectrum. This is particularly obvious for energies >2 MeV, as shown in Fig. 5. Thus, the increase in the fast fluxes in the ELXSIR-OLD analysis is caused by a combination of a better energy representation in the fast energy range and a slightly harder neutron source fission spectrum. Incidentally, the 56-energy-group fission spectrum that was used in the ELXSIR transport analyses was recommended by Ref. 8 for such calculations.

As fast neutrons penetrate the pressure vessel wall, the relative difference between the fast fluxes of the two libraries (BUGLE-80 and ELXSIR-OLD) increased to 17 and 31% at the pressure vessel outer wall surface for energies >1.0 and 0.1 MeV, respectively. This large difference in the fast flux through the pressure vessel wall is attributed to the high fast flux in the core region. This is shown in Fig. 6, where the ELXSIR (56-group) neutron spectrum at the pressure vessel inner wall surface is clearly harder than that of BUGLE-80 (47-group) for energies between 0.1 and 10 MeV.

As expected, when the updated iron cross sections are used, the relative difference between the fast fluxes calculated using BUGLE-80 and ELXSIR remained approximately the same in the core region, while it almost doubled to 17% in the core barrel and downcomer regions. This increase in the fast flux is obviously due to the interaction of fast neutrons with iron in the core shroud and core barrel. As fast neutrons penetrate the pressure vessel wall, the relative difference increased to 43 and 35% at the pressure vessel outer wall surface for energies >1.0 and 0.1 MeV, respectively. It is important to note that in order to get an accurate measure of the effect of the updated iron cross sections on the fast flux, a comparison should be made between the results of the two ELXSIR analyses. For example, the updated iron cross sections increased the fast flux ($E > 1.0$ MeV) at the SONGS-2 pressure vessel inner and outer wall surfaces by ~11 and 22%, respectively, as shown in Fig. 7. Figure 7 shows the relative difference in the fast flux ($E > 1.0$ MeV) for the SAILOR,

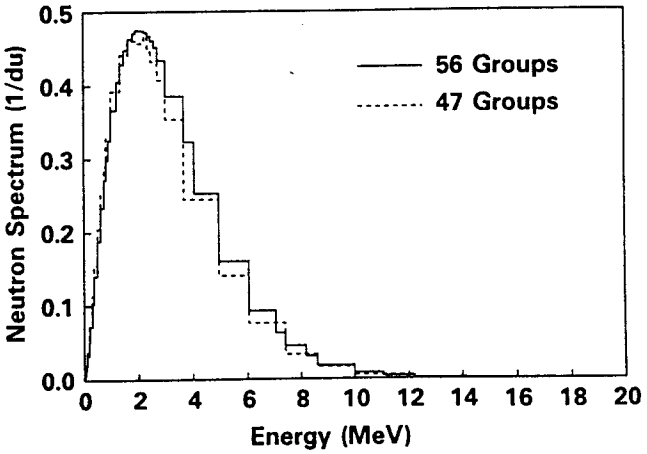

Fig. 5. The 56- and 47-energy-group neutron source fission spectra for SONGS-2.

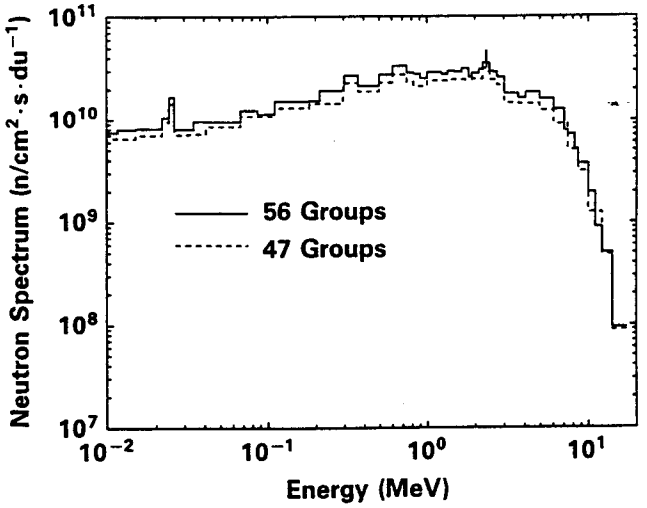

Fig. 6. The ELXSIR and BUGLE-80 neutron spectra at the pressure vessel inner wall surface for SONGS-2.

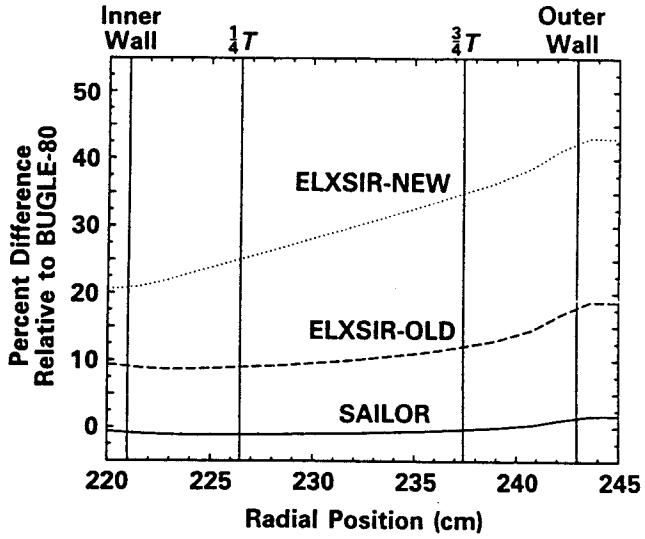

Fig. 7. A comparison of the relative difference in the fast flux ($E > 1.0$ MeV) for SAILOR, ELXSIR-NEW, and ELXSIR-OLD within the SONGS-2 pressure vessel wall.

TABLE III

Comparison of the Fast Flux ($E > 1.0$ MeV) C/E Ratios at the SONGS-2 97-deg In-Vessel Surveillance Capsule

Reaction	C/E[a]	C/E[b]	C/E[c]	C/E[d]
$^{54}Fe(n,p)^{54}Mn$	0.72	0.87	0.84	0.76
$^{58}Ni(n,p)^{58}Co$	0.69	0.87	0.84	0.77
$^{63}Cu(n,\alpha)^{60}Co$	0.76	0.83	0.76	0.73
$^{46}Ti(n,p)^{46}Sc$	0.82	1.00	0.94	0.87

[a]BUGLE-80 and SAILOR cross-section libraries with a mixed core fission source spectrum (83.5% ^{235}U and 16.5% ^{239}Pu).
[b]ELXSIR cross-section library with the updated iron cross sections and a mixed core fission source spectrum (83.5% ^{235}U and 16.5% ^{239}Pu).
[c]ELXSIR cross-section library with the updated iron cross sections and a pure ^{235}U core fission source spectrum.
[d]ELXSIR cross-section library with the original iron cross sections and a mixed core fission source spectrum (83.5% ^{235}U and 16.5% ^{239}Pu).

ELXSIR-NEW, and ELXSIR-OLD cross-section libraries. In these plots, BUGLE-80 results were used as the reference point.

This increase in the fast flux from the core barrel out to the cavity region is due mainly to an ~10% reduction in the inelastic cross sections of iron in the energy range between 3 and 12 MeV and to the introduction of a forward-peaked angular distribution in the inelastic differential scattering kernel.[20] Iron is obviously the major constituent of the core barrel, pressure vessel wall, and cladding materials.

Since the objective is to determine the uncertainty in the calculated fluxes, C/E ratios at particular dosimetry positions were studied. Table III shows the C/E ratios for several fast threshold reactions at the 97-deg in-vessel surveillance capsule of SONGS-2. As seen in Table III, use of updated iron cross sections resulted in C/E ratios to within 17% of unity compared with 31% of unity for both BUGLE-80 and SAILOR. This result is very significant since it shows that the ENDF/B-V Mod 3 iron cross sections tend to improve the C/E ratios and bring them closer to unity. Furthermore, the C/E ratios calculated using the original iron cross sections, as shown in Table III, are within 24% of unity. This shows that the original iron cross sections in ELXSIR will underpredict the fast neutron flux at the pressure vessel inner wall surface by as much as 15% when compared with that calculated using the updated iron cross sections. This 15% difference in the C/E ratios represents the effect of the Fu and Hetrick modification to the iron cross sections on the calculated fast flux at the pressure vessel inner wall surface.

Additionally, the effect of the neutron source fission spectrum in the core region on the calculated fluxes at the pressure vessel inner wall surface is also shown in Table III. When a pure ^{235}U fission spectrum is used to represent the neutron source in the core region, it can underpredict the fast flux at the pressure vessel inner wall surface by as much as 9% compared with a more representative mixed spectrum. Thus, an accurate representation of the fission spectrum should account for the presence of ^{239}Pu in the core, especially when highly burned fuel assemblies are being used. That is because there are roughly 30% more 10-MeV neutrons from the thermal fission of ^{239}Pu than from ^{235}U, as clearly shown in Fig. 8.

The vessel eccentricity was modeled by moving the core and core barrel 1.27 cm closer to the pressure vessel wall. The fast fluxes at the azimuthal peak position were calculated using the ELXSIR cross-section library with the updated iron cross sections. The fast fluxes for both energy cutoffs were ~17% higher through the pressure vessel wall. This increase is significant because it shows that relatively small as-built eccentricities can result in a greater uncertainty in the calculated fast fluxes through the pressure vessel wall than that due to the cross-section library being used. It is important to note that the 1.27 cm used in the analysis was chosen after extensive examination of plant drawings for several PWRs and boiling water reactors (BWRs). Several of these drawings showed that the inner radius of the pressure vessel wall can vary by as much as 0.5 cm or more, depending on the axial elevation. Additionally, it is believed[28] that the pressure vessel wall out-of-roundness can contribute to variation in the pressure vessel wall design radius by as much as ±1.0 cm (pressure vessel wall thickness is constant). There were also

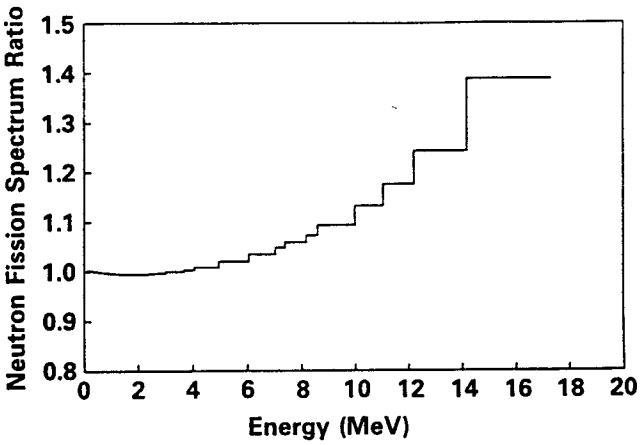

Fig. 8. The ratio of a mixed fission spectrum (16.5% ^{239}Pu and 83.5% ^{235}U) to that of a pure ^{235}U fission spectrum.

some uncertainties in the dimensions of the core shroud and core barrel. Thus, based on engineering judgment, we assumed that the combined effect of these factors can produce a pressure vessel eccentricity of 1.27 cm (0.5 in.) (i.e., less water between the core and the pressure vessel wall). However, realistically, the combined effect of these factors may be quite different from what we have reported here, depending on the actual design and/or construction of these components.

The calculated reaction rates for several fast threshold reactions are shown in Table IV at the SONGS-2 97-deg surveillance capsule for BUGLE-80, SAILOR, ELXSIR-NEW, ELXSIR-OLD, and ELXSIR-NEW with a ^{235}U fission spectrum to represent the neutron source in the core region. The maximum difference occurred for the ^{58}Ni, ^{54}Fe, and ^{46}Ti reactions, which have threshold energies of 2.1, 2.3, and 3.9 MeV, respectively, and was between the ELXSIR-NEW and BUGLE-80 results. These differences are 25, 26.2, and 23.3%, respectively. On the other hand, the reaction rates were on average 15% higher for ELXSIR-NEW compared with that of ELXSIR-OLD, while the fast neutron flux ($E > 1.0$ MeV) was 10.4% higher.

The new and old iron dpa cross sections in 620-energy-group structure are compared in Figs. 9 and 10. Also shown in these figures are the iron dpa cross sections found in the ELXSIR library and the new iron dpa cross sections collapsed to ELXSIR 56-energy-group structure using the Watt spectrum. As seen in these figures, the two fine dpa cross sections are identical for energies >0.03 MeV and for energies <10 eV, while they were somewhat different for energies in between. However, the absolute magnitude of the dpa cross sections in the latter region ranges from 0.1 to 20 b compared with thousands and hundreds of barns in the other two regions. Similarly, the old and new

TABLE IV

Comparison of Reaction Rates* for Several Fast Threshold Reactions at the SONGS-2 97-deg In-Vessel Surveillance Capsule

Reaction	BUGLE-80[a]	SAILOR[a]	ELXSIR[b]	ELXSIR[c]	ELXSIR[d]
	Reaction Rates [(n/s) × 10^{10}]				
^{238}U(n,f)	2.1300	2.1200	2.5800	2.5000	2.3200
^{237}Np(n,f)	11.200	11.200	12.900	12.600	11.200
^{58}Ni(n,p)^{58}Co	0.7850	0.7780	0.9840	0.9440	0.8650
^{54}Fe(n,p)^{54}Mn	0.6080	0.6020	0.7670	0.7340	0.6710
^{46}Ti(n,p)^{46}Sc	0.1160	0.1150	0.1430	0.1340	0.1240
^{63}Cu(n,α)^{60}Co	0.0083	0.0082	0.0091	0.0083	0.0079
	Neutron Flux [(n/cm^2·s) × 10^{10}]				
$\phi(E > 0.1)$	9.1500	9.1300	10.900	10.700	10.000
$\phi(E > 1.0)$	4.7500	4.7200	5.7300	5.5800	5.1900

*At the capsule middle compartment (3 in. above core midplane).
[a]Mixed core fission source spectrum (83.5% ^{235}U and 16.5% ^{239}Pu).
[b]ELXSIR cross-section library with the updated iron cross sections and a mixed core fission source spectrum (83.5% ^{235}U and 16.5% ^{239}Pu).
[c]ELXSIR cross-section library with the updated iron cross sections and a pure ^{235}U core fission source spectrum.
[d]ELXSIR cross-section library with the original iron cross sections and a mixed core fission source spectrum (83.5% ^{235}U and 16.5% ^{239}Pu).

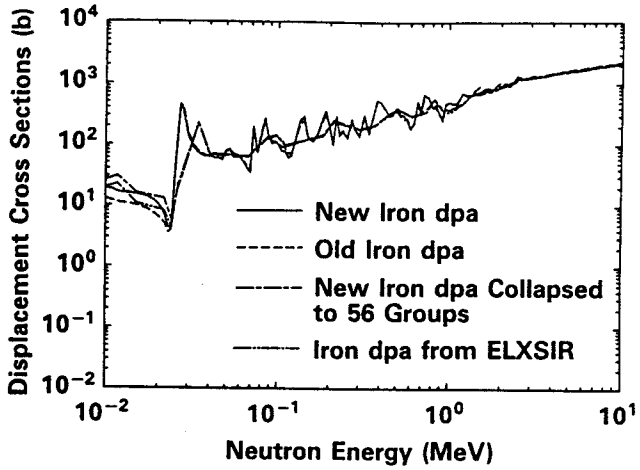

Fig. 9. Comparison of the iron dpa cross sections for $E >$ 0.01 MeV.

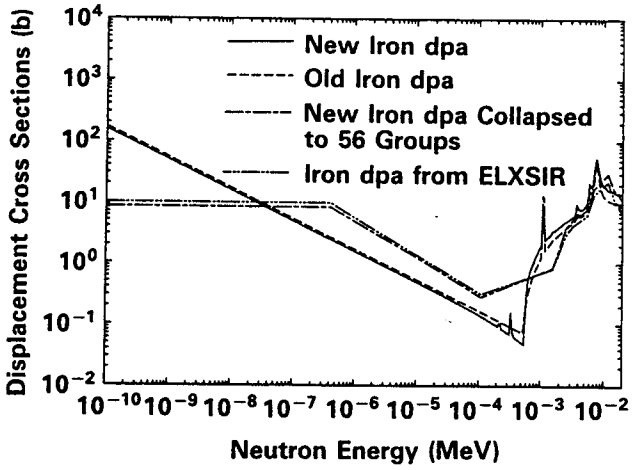

Fig. 10. Comparison of the iron dpa cross sections for $E <$ 0.01 MeV.

coarse dpa cross sections are roughly the same throughout the energy range. This can also be seen in Fig. 11, where the total dpa per second for the new and old iron dpa cross sections (56 groups) are compared through the SONGS-2 pressure vessel wall.

The NRC attenuation functions proposed in Ref. 26 were compared through the pressure vessel wall of SONGS-2 with the calculated fast flux and dpa per second. It was found that the attenuation of the calculated fast flux and dpa per second was less rapid than the functions proposed in Ref. 29, as shown in Fig. 12. Reference 29 shows that the Revision 2 formula is overly conservative for the small German BWR, which has a pressure vessel wall thickness of only 5 in. Thus, there might be a correlation between the appropriateness of the proposed formulas in Ref. 26 and the type of the reactor and/or pressure vessel wall thickness.

In addition, a study of the azimuthal dependence of the dpa attenuation though the pressure vessel wall was also performed. This information is important in determining the need for azimuthally dependent dpa attenuation models. Several critical angles were chosen for plotting the pressure vessel wall dpa attenuation, as shown in Fig. 13. These critical angles were chosen at azimuthal positions where the largest neutron spectral variation is expected to occur. Referring to Fig. 2,

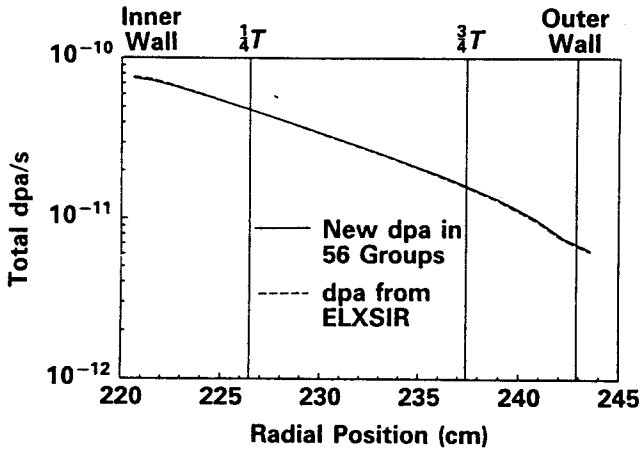

Fig. 11. The radial profile of the total dpa per seconds through the pressure vessel wall of SONGS-2.

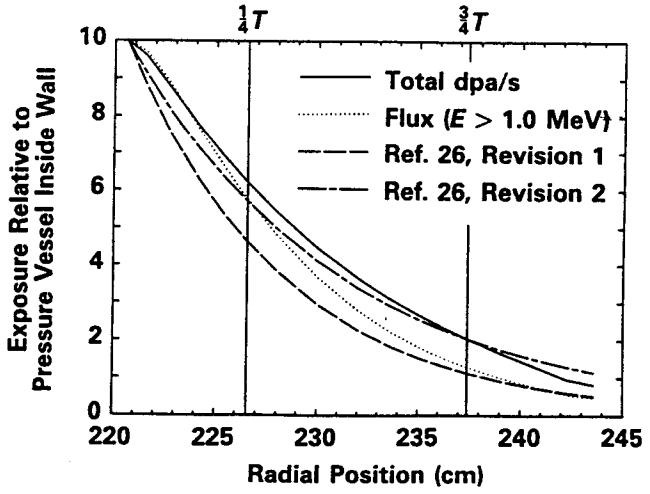

Fig. 12. A comparison of the attenuation of several key exposure parameters through the pressure vessel wall of SONGS-2.

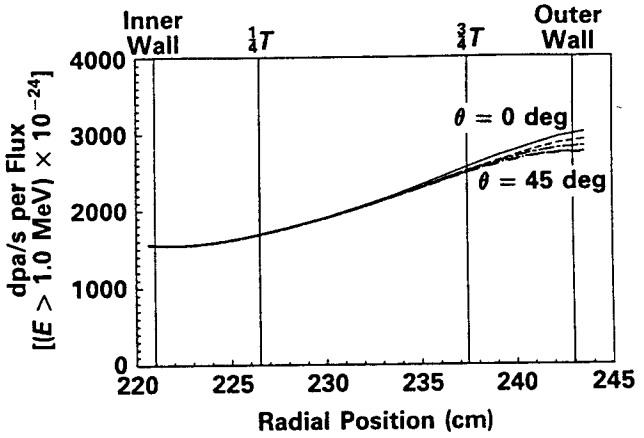

Fig. 13. A comparison of the quantity (dpa per second/fast flux) through the SONGS-2 pressure vessel wall for several azimuthal angles.

these angles correspond to the peak flux angle (θ = 0 deg), fuel corner angle near maximum water traverse (θ = 9 deg), maximum water traverse angle (θ = 10 deg), fuel corner angle (θ = 39 deg), and large water traverse angle (θ = 45 deg). As seen in Fig. 13, the azimuthal dependence is negligible at the $\frac{1}{4}T$ and $\frac{3}{4}T$ positions for this reactor. Nevertheless, future studies should focus on addressing this concern in a comprehensive manner.

IV.B. Reactor X Transport Results

The trends observed in the SONGS-2 analysis with regard to the fast flux and energy spectra calculations were also observed in Reactor X analysis. For example, the SAILOR-calculated synthesized three-dimensional fast fluxes with energies >1.0 and 0.1 MeV were nearly identical (~1.0%) to those obtained using BUGLE-80 out to the pressure vessel inner wall surface (218.34 cm). As fast neutrons traverse through the pressure vessel wall, the SAILOR-calculated fast flux with energy >0.1 MeV was 2.88% higher at the pressure vessel outer wall surface. These results are similar to those obtained in Sec. IV.A. Once again, the difference in the fast flux through the pressure vessel wall is caused by the $\frac{1}{4}T$ weighting spectrum that was used to generate SAILOR iron cross sections. What is interesting in these findings is that even though SAILOR was generated using more representative weighting spectra, it produced results (fast flux) that are relatively similar to those of BUGLE-80.

As expected, the fast fluxes (E > 1.0 and 0.1 MeV) calculated using ELXSIR-OLD and ELXSIR-NEW were once again considerably higher than those calculated using the BUGLE-80 library. Using the original iron cross sections, the calculated fast fluxes for both energy cutoffs were ~8 and 9% higher in the core region and in the core barrel and downcomer regions, respectively. As fast neutrons penetrate the pressure vessel wall, the relative difference between the fast fluxes of the two libraries increased to 16 and 29% at the pressure vessel outer wall surface for energies >1.0 and 0.1 MeV, respectively, as was the case in SONGS-2.

When the updated iron cross sections are used, the relative difference between the fast fluxes calculated using BUGLE-80 and ELXSIR remained essentially the same in the core region, while it increased to ~16% in the core barrel and downcomer regions for both energy cutoffs. These results are once again similar to those reported in Sec. IV.A. As fast neutrons penetrate the pressure vessel wall, the relative difference at the pressure vessel outer wall surface remained the same for E > 0.1 MeV (29%), while it increased to 37% for E > 1.0 MeV. Figure 14 shows the radial distribution of the relative difference in the fast flux (E > 1.0 MeV) for the three libraries. Again, BUGLE-80 results were used as the reference point in these plots.

Table V shows the C/E ratios for several fast threshold reactions at the 90-deg (near core midplane) and 97-deg (~81 cm above core midplane) ex-vessel dosimetry locations of Reactor X. Once again, the use of ELXSIR-NEW resulted in increased C/E ratios for both dosimetry locations. These results show that the updated iron cross sections tend to increase the transmission of fast neutrons through the pressure vessel wall. Further, the C/E ratios calculated using the ELXSIR-OLD cross sections, shown in Table V, are

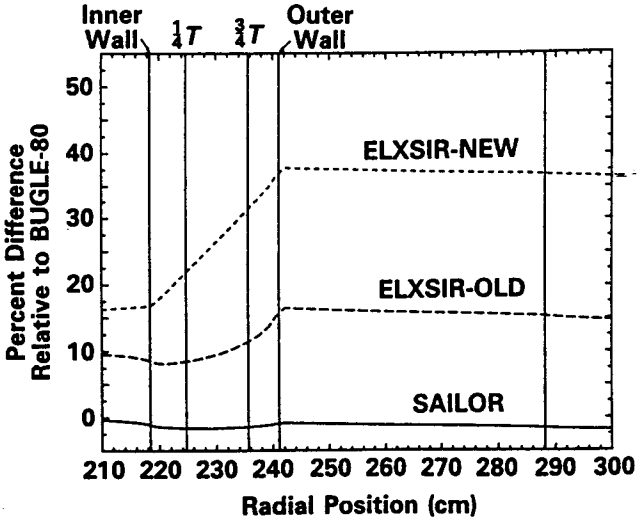

Fig. 14. A comparison of the relative difference in the fast flux (E > 1.0 MeV) for SAILOR, ELXSIR-NEW, and ELXSIR-OLD within the Reactor X pressure vessel wall.

TABLE V

Comparison of the Fast Flux ($E > 1.0$ MeV) C/E Ratios for Reactor X Ex-Vessel Dosimetry Locations

Reaction	C/E[a]	C/E[b]	C/E[c]	C/E[d]	C/E[e]
90-deg Cavity Dosimetry (near core midplane)					
$^{54}Fe(n,p)^{54}Mn$	1.020	1.035	1.675	1.584	1.140
$^{58}Ni(n,p)^{58}Co$	1.028	1.042	1.667	1.578	1.160
$^{63}Cu(n,\alpha)^{60}Co$	1.234	1.230	1.669	1.443	1.125
97-deg Cavity Dosimetry (~81 cm above core midplane)					
$^{54}Fe(n,p)^{54}Mn$	1.080	1.088	1.770	1.667	1.208
$^{58}Ni(n,p)^{58}Co$	1.102	1.109	1.780	1.680	1.246
$^{63}Cu(n,\alpha)^{60}Co$	1.269	1.259	1.710	1.472	1.158

[a]BUGLE-80 cross-section library with a mixed core fission source spectrum (80% ^{235}U and 20% ^{239}Pu).
[b]SAILOR cross-section library with a mixed core fission source spectrum (80% ^{235}U and 20% ^{239}Pu).
[c]ELXSIR cross-section library with the updated iron cross sections and a mixed core fission source spectrum (80% ^{235}U and 20% ^{239}Pu).
[d]ELXSIR cross-section library with the updated iron cross sections and a pure ^{235}U core fission source spectrum.
[e]ELXSIR cross-section library with the original iron cross sections and a mixed core fission source spectrum (80% ^{235}U and 20% ^{239}Pu).

on average 40% lower than those of ELXSIR-NEW. This large difference is attributed to the Fu and Hetrick modification of the iron cross sections.

It is interesting to note that the C/E ratios for ELXSIR-NEW are much higher than unity for both dosimetry locations (90 and 97 deg). One reason for this is that the ELXSIR-NEW cross sections have a higher fast neutron transmission probability and the fact that the C/E ratios for BUGLE-80 and SAILOR were above unity to begin with. A second reason for this is the harder fission spectrum that was used to model the neutron source in the core region. This is evident in ELXSIR-OLD C/E ratios since these ratios should be closer to those of BUGLE-80 and SAILOR. The most interesting result from Table V is that the C/E ratios for BUGLE-80 and SAILOR were greater than unity for both the 90-deg cavity dosimetry, which is located near the core midplane, and the 97-deg cavity dosimetry, located ~81 cm above core midplane. One explanation for this is the fact that as-built data were used for most of the components. Also, we believe that there is some vessel eccentricity in Reactor X.

The effect of the neutron source fission spectrum in the core region on the calculated flux at the pressure vessel outer wall surface is also reported in Table V.

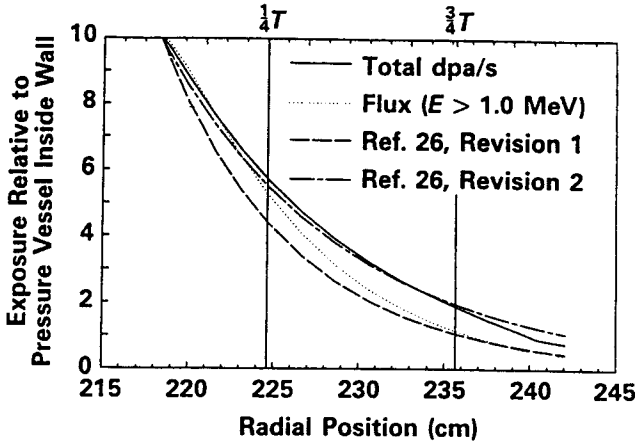

Fig. 15. A comparison of the attenuation of several key exposure parameters through the pressure vessel wall of Reactor X.

When a pure ^{235}U fission spectrum is used to represent the neutron source in the core region, it can underpredict the fast flux at the pressure vessel outer wall surface by as much as 15%, as shown in Table V for the ^{63}Cu fast reaction. The attenuation of the calculated dpa per second through the pressure vessel wall of Reactor X differs from the proposed dpa equivalent attenuation formula in Ref. 26, Revision 2, as shown in Fig. 15. This seems to provide additional support to the argument that dpa calculations should be performed through the pressure vessel wall whenever possible because the dpa equivalent attenuation formula in Ref. 26, Revision 2, can be inappropriate for certain plants.

The reaction rates of several fast threshold reactions at the 90-deg ex-vessel dosimetry positions of Reactor X are shown in Table VI for BUGLE-80, SAILOR, ELXSIR-NEW, ELXSIR-OLD, and ELXSIR-NEW with a pure ^{235}U neutron source fission spectrum. As in SONGS-2, the maximum difference occurred for the ^{58}Ni, ^{54}Fe, and ^{46}Ti threshold reactions. The average difference between BUGLE-80 and ELXSIR-NEW for these reactions was 63%, while it was 44% between ELXSIR-NEW and ELXSIR-OLD. On the other hand, the fast flux ($E > 1.0$ MeV) calculated using ELXSIR-NEW was 37.5 and 19% higher than those calculated using BUGLE-80 and ELXSIR-OLD, respectively.

V. SUMMARY AND CONCLUSIONS

Neutron transport analyses were performed for the SONGS-2 and Reactor X PWRs using three multigroup cross-section libraries developed for LWR shielding and pressure vessel surveillance dosimetry applications. The synthesized three-dimensional neutron fluxes and

TABLE VI

Comparison of the Reaction Rates* for Several Fast Threshold Reactions at Reactor X 90-deg Ex-Vessel Dosimetry Locations

Reaction	BUGLE-80[a]	SAILOR[a]	ELXSIR-NEW[b]	ELXSIR-NEW[c]	ELXSIR-OLD[d]
	Reaction Rates [(n/s) × 10^8]				
$^{238}U(n,f)$	3.2000	3.2100	4.5500	4.3700	3.6100
$^{237}Np(n,f)$	48.500	49.900	63.200	61.200	60.700
$^{58}Ni(n,p)^{58}Co$	0.8030	0.8080	1.2900	1.2300	0.9060
$^{54}Fe(n,p)^{54}Mn$	0.5930	0.5970	0.9680	0.9160	0.6620
$^{46}Ti(n,p)^{46}Sc$	0.1180	0.1180	0.1910	0.1770	0.1250
$^{63}Cu(n,\alpha)^{60}Co$	0.0100	0.0099	0.0135	0.0122	0.0091
	Neutron Flux [(n/cm^2·s)] × 10^8]				
$\phi(E > 0.1)$	94.000	95.500	122.00	119.00	123.00
$\phi(E > 1.0)$	10.400	10.300	14.300	13.800	12.000

*At the capsule middle compartment (core midplane).
[a]Mixed core fission source spectrum (80% ^{235}U and 20% ^{239}Pu).
[b]ELXSIR cross-section library with the updated iron cross sections and a mixed core fission source spectrum (80% ^{235}U and 20% ^{239}Pu).
[c]ELXSIR cross-section library with the updated iron cross sections and a pure ^{235}U core fission source spectrum.
[d]ELXSIR cross-section library with the original iron cross sections and a mixed core fission source spectrum (80% ^{235}U and 20% ^{239}Pu).

energy spectra were calculated by synthesizing the r-θ and r-z results using the z normalization model. The synthesized three-dimensional neutron fluxes and energy spectra were calculated at the pressure vessel inner wall surface, $\frac{1}{4}T$, $\frac{3}{4}T$, outer wall surface, and cavity region. The C/E ratios and reaction rates for several fast reactions were calculated at the SONGS-2 97-deg in-vessel surveillance capsule and at Reactor X 90- and 97-deg (C/E ratios only) ex-vessel dosimetry locations. The results obtained using the BUGLE-80 and SAILOR libraries for the fast neutron flux ($E > 1.0$ and 0.1 MeV) were in good agreement out to the pressure vessel inner wall surface for both reactors. Using the SAILOR library, the fast fluxes ($E > 0.1$ MeV) leaving the pressure vessel wall was 5.5 and 2.9% higher for SONGS-2 and Reactor X, respectively.

In the case of the ELXSIR library, the fast fluxes were much higher in the core region and considerably higher in the downcomer and through the pressure vessel wall for both reactors. For the original iron cross sections, the fast flux ($E > 1.0$ MeV) was ~8% higher than that of BUGLE-80 in both the core region and the downcomer for both reactors. It increased to ~17% at the pressure vessel outer wall surface for both reactors. When the updated iron cross sections were used, the difference in the fast flux ($E > 1.0$ MeV) remained essentially the same in the core region, while it increased from 8 to 17% in the downcomer for both reactors. The difference in the fast flux ($E > 1.0$ MeV) increased to 43 and 37% at the pressure vessel outer wall surface for SONGS-2 and Reactor X, respectively.

The C/E ratios calculated using ELXSIR for SONGS-2 were close to unity while those calculated using the other two cross-section libraries were ~0.78. In the case of Reactor X, the C/E ratios calculated using BUGLE-80 and SAILOR were close to unity, while the ELXSIR-NEW calculated C/E ratios were much higher (~1.7). The reaction rates calculated using ELXSIR with the updated iron cross sections were on average 25 and 63% higher than those of BUGLE-80 for SONGS-2 and Reactor X, respectively, at the corresponding dosimetry locations. The fast flux ($E > 1.0$ MeV) through the pressure vessel wall increased by 17% when the SONGS-2 core and core barrel were moved 1.27 cm closer to the pressure vessel wall to simulate vessel eccentricity. The mixed fission spectrum (^{239}Pu and ^{235}U) produced higher fast neutron flux through the pressure vessel wall by as much as 10% for SONGS-2 and 15% for Reactor X. The new and old iron dpa cross sections were nearly identical in the energy range of interest. Finally, with regard to the pressure vessel wall dpa attenuation, the Ref. 26, Revision 2 dpa equivalent attenuation formula differed from the plant-specific calculation for both SONGS-2 and Reactor X.

This study outlined the important differences in the neutron fluxes and spectra calculated using the cross-section libraries BUGLE-80, SAILOR, and ELXSIR.

We believe that BUGLE-80 and SAILOR libraries can be considered adequate for pressure vessel dosimetry studies with the knowledge that they can and in most cases do underpredict the fast fluxes through the pressure vessel wall of a PWR by as much as 30%. However, failure to model the as-built configuration of the various components inside the pressure vessel wall, as well as the source distribution and power history, can overshadow the uncertainty associated with the cross-section library. Based on the measured dosimetry data and C/E ratios, we conclude that the ELXSIR cross-section library is the most suitable library for broad multigroup LWR pressure vessel calculations. This is because it contains the latest version of the Fu and Hetrick iron cross sections available in a format suitable for ANISN or DOT calculations. Additionally, we recommend that dpa calculations be performed to the extent practical in order to obtain actual dpa attenuation through the pressure vessel wall rather than relying solely on the generic attenuation formulas.

ACKNOWLEDGMENTS

We would like to acknowledge Southern California Edison Company for permitting us to use their transport data to perform this study. Also, we would like to acknowledge the computer center at the Pennsylvania Sate University for their valuable assistance during the installation of some of the computer software that was used to perform the calculations and for providing us with needed computer time to complete our study.

REFERENCES

1. "Practice for Effects of High-Energy Neutron Radiation on the Mechanical Properties of Metallic Materials," ASTM E184, American Society for Testing and Materials.

2. A. FABRY, et al., "Improvement of LWR Pressure Vessel Steel Embrittlement Surveillance (1982–1983), Progress Report on Belgian Activities in Cooperation with the USNRC and other R&D Programs," *Proc. 5th Symp. Reactor Dosimetry* (1984).

3. "Method for Determining Neutron Flux, Fluence, and Spectra by Radioactivation Techniques," ASTM E261, American Society for Testing and Materials.

4. "Method for Determining Thermal Neutron Flux by Radioactivation Techniques," ASTM E262, American Society for Testing and Materials.

5. M. P. MANAHAN and H. S. BASHA, "Flux and Fluence Determination Using the Material Scrapings Approach," *J. of Nucl. Technol.*, **93**, 389 (1991).

6. "Bugle 80 Coupled 47 Neutron, 20 Gamma, P_3 Cross-Section Library for LWR Shredding Calculations," DLC-75, Oak Ridge National Laboratory (1980).

7. G. L. SIMMONS and R. ROUSSIN, "SAILOR—A Coupled Cross Sections Library for Light Water Reactors," DLC-76/SAILOR, Reactor Shielding Information Center, Oak Ridge National Laboratory (Mar. 1983).

8. R. E. MAERKER and W. E. FORD, "The ELXSIR Cross Section Library for LWR Pressure Vessel Irradiation Studies: Part of the LEPRICON Computer Code System," EPRI NP-3654, Electric Power Research Institute (Sep. 1984).

9. E. A. STRAKER, G. W. MORRISON, and R. H. ODEGAARDEN, "A Coupled Neutron and Gamma-Ray Cross Section Library for Use in Shielding Calculations," *Trans. Am. Nucl. Soc.*, **15**, 535 (1972).

10. W. E. FORD III and D. H. WALLACE, "POPOP4, A Code for Converting Gamma-Ray Spectra to Secondary Gamma-Ray Production Cross Sections," CTC-12 (1960).

11. D. E. BARTINE et al., "Production and Testing of the DNA Few Group Cross Section Library," ORNL/TM/4840, Oak Ridge National Laboratory (1975).

12. W. E. FORD III et al., "A 218-Group Neutron Cross Section Library in the AMPX Master Interface Format for Criticality Safety Studies," ORNL/CSD/TM-4, Oak Ridge National Laboratory (1976).

13. J. A. BUCHOLZ, "SCALE: A Modular Code System for Performing Standardized Computer Analyses for Licensing Evaluation," NUREG/CR-0200, ORNL/NUREG/CSD-2, Vol. I, U.S Nuclear Regulatory Commission.

14. J. T. WEST et al., "Developing an ANS Coupled Cross-Section Standard for Concrete Shielding," *Trans. Am. Nucl. Soc.*, **28**, 642 (1978).

15. "BUGLE Coupled 45 Neutron, 16 Gamma, P_3 Cross Sections for Studies by ANSI 6.1.2 Shielding Standards Working Group on Multigroup Cross Sections, Informal Notes," DLC-47/BUGLE, Reactor Shielding Information Center, Oak Ridge National Laboratory (1977).

16. R. W. ROUSSIN et al., "VITAMIN-C: The CTR Processed Multigroup Cross Section Library for Neutronics Studies," ORNL-RSIC-37, Oak Ridge National Laboratory (1980).

17. "Guide for Application of Neutron Transport Methods for Reactor Vessel Surveillance," ASTM E482, American Society for Testing and Materials.

18. W. A. RHOADES and R. L. CHILDS, "An Updated Version of DOT IV, One- and Two-Dimensional Neutron-Photon Transport Code," DOT IV Version 4.3, ORNL-5851, Oak Ridge National Laboratory (1982).

19. R. W. ROUSSIN et al., "VITAMIN-E: A Coupled 174 neutron, 39 Gamma-Ray Multigroup Cross-Section Library for Deriving Application-Dependent Working Libraries for Radiation Transport Calculations," ORNL-RSIC, Oak Ridge National Laboratory (1984).

20. C. Y. FU and D. M. HETRICK, "Update of ENDF/B-V Mod-3 Iron: Neutron-Producing Reaction Cross Sections and Energy-Angle Correlations," ORNL/TM-9964, Oak Ridge National Laboratory (July 1986).

21. R. JUNG, R. S. DENNINGS, and M. P. MANAHAN, "The Development of Pre and Post Transport Analysis Codes: PINPOW, FMAT, and FLUX3DSYN," Internal Report, Battelle Memorial Institute (Oct. 1983).

22. P. CHOWDHURY et al., "Development of a Three-Dimensional Flux Synthesis Program and Comparison with 3-D Transport Theory Results," ORNL/TM-10503, Oak Ridge National Laboratory (Jan. 1988).

23. F. B. K. KAM et al., "Pressure Vessel Analysis and Neutron Dosimetry," ORNL/TM-10651, Oak Ridge National Laboratory (Nov. 1987).

24. M. B. DANJAJI and J. G. WILLIAMS, *Displacement Cross Sections for Neutron Interactions in Ferritic Steel*, University of Illinois (1991).

25. "Practice for Characterizing Neutron Exposures in Ferritic Steels in Terms of Displacements per Atom (DPA)," ASTM E693-79, American Society for Testing and Materials.

26. "Radiation Embrittlement of Reactor Vessel Material," Regulatory Guide 1.99, Revisions 1 and 2, U.S. Nuclear Regulatory Commission.

27. "DOSDAM84 Multigroup Cross Sections In SAND-II Format for Spectral Integral, and Damage Analysis," DLC-131, Radiation Shielding Information Center, Oak Ridge National Laboratory (Oct. 1987).

28. "Application of the LEPRICON Methodology to the Arkansas Nuclear One, Unit 1 Reactor," Interim Report, Electric Power Research Institute (Feb. 1986).

29. G. PRILLINGER, "Neutron Exposure of Gundremmingen—A Pressure Vessel Trepans, Reactor Dosimetry: Methods, Applications, and Standardization," ASTM STP 1001, American Society for Testing and Materials (1989).

Hassan S. Basha (BSc, nuclear engineering, University of Michigan, 1986; MSc, nuclear engineering, Ohio State University) is a PhD candidate and research assistant in the Nuclear Engineering Department at Pennsylvania State University (PSU). His current research interests include plant life extension, radiation transport analysis, reactor dosimetry and shielding analysis, neutron activation analysis, and boron capture therapy.

M. P. Manahan, Sr. (BS, mathematics and BA, physics, Michigan State University, 1975; MS, reactor physics, Columbia University, 1978; ScD, nuclear materials engineering, Massachusetts Institute of Technology, 1982) is an adjunct professor at PSU and president of MPM Research & Consulting. His current research interests include plant life extension, miniaturized specimen technology, radiation transport analysis, pressure vessel surveillance, and computer-based technology management.